THE JOURNAL OF PHYSICAL CHEMISTRY B LETTERS

**2006,** *110,* 46−49
Published on Web 12/09/2005

# Identification of Color Centers on MgO(001) Thin Films with Scanning Tunneling Microscopy

**Martin Sterrer,*,† Markus Heyde,† Marek Novicki,‡ Niklas Nilius,† Thomas Risse,† Hans-Peter Rust,† Gianfranco Pacchioni,§ and Hans-Joachim Freund†**

*Fritz-Haber-Institut der Max-Planck-Gesellschaft, Department of Chemical Physics, Faradayweg 4-6, D-14195 Berlin, Germany, University of Wroclaw, Institute of Experimental Physics, Pl. Maxa Borna 9, PL-50-204 Wroclaw, Poland, and Universita degli Studi Milano-Bicocca, Dipartimento di Scienza dei Materiali, via R. Cozzi, I-53-20125 Milano, Italy*

*Received: November 1, 2005; In Final Form: November 18, 2005*

Localized electronic defects on the surface of a 4 monolayer (ML) thin MgO(001) film deposited on Ag(001) have been investigated by low-temperature scanning tunneling microscopy and spectroscopy. Depending on the location of the defect, we observe for the first time different defect energy levels in the band gap of MgO. The charge state of defects can be manipulated by interactions with the scanning tunneling microscope tip. Comparison with ground state energy levels of color centers on the MgO surface obtained from embedded cluster calculations corroborates the assignment of the defects to singly and doubly charged color centers.

Color centers (F centers) are a prototypic example for point defects in the alkaline earth metal oxides. Their properties have been studied extensively in the past decades both experimentally and theoretically. In early experiments on heavily bombarded MgO single crystals, electron paramagnetic resonance[1] and optical absorption studies[2] have proven the existence of bulk color centers, that is, oxygen vacancies occupied by one ($F^+$) or two ($F^0$) electrons. These experimental methods have also been used to detect color centers located on the surface of MgO powder, where so-called $F_S^+$(H) centers, consisting of an electron stabilized by a nearby OH group, have been studied extensively. There has been controversial discussion on the possible location of these defects over the past decades, ranging from oxygen vacancies on the (100) terrace[3], to low coordinated oxygen vacancies at edges or corners,[4] and to the most recent conclusion that ($H^+$)($e^-$) pairs are the most abundant defects and oxygen vacancies play only a minor role.[5−8] Apart from studies on $F_S^+$(H) centers, there is only little experimental evidence that electrons may be trapped on the surface of MgO powder without the stabilizing effect of a neighboring OH group.[9]

A detailed understanding of these surface defects is highly desirable not the least because of the suggested role of color centers as active sites in catalysis. This fact was recently boosted by studies, which, from a combination of indirect experimental evidence and theoretical calculations, infer the involvement of color centers for the enhanced catalytic activity of deposited metal particles.[10] Despite the debate on a possible role of charged defects in catalysis, the geometric and electronic details of surface color centers are widely discussed. In particular, the electronic properties of differently charged color centers at various surface locations (e.g., anion vacancies on a terrace, step, or corner as well as divacancies and kinks) are now accessible from calculations.[11−14] However, detailed experimental investigations to corroborate these results are scarce.[15] This is due to the fact that the manifold of sites located at different positions and exhibiting different charge states leads to highly convoluted signals for most spectroscopic methods, which are often difficult to disentangle. To gain both morphological and spectroscopic information on single color centers on a microscopic level, we aim in this study at a local microscopic and spectroscopic characterization of these defects on the surface of MgO thin films using low-temperature scanning tunneling microscopy (STM).

Progress in the morphological characterization of MgO surfaces has recently been achieved by the use of scanning probe techniques. Large terraces as well as vacancy defects are observed on MgO(100) single crystal surfaces by noncontact atomic force microscopy (NC-AFM).[16,17] STM applied to MgO-(001) thin films grown on Ag(001) revealed the growth mechanism of MgO films and showed the possibility for an electronic characterization by scanning tunneling spectroscopy (STS).[18−20] Already after the completion of 3 monolayers (ML), the development of a bulklike electronic structure with a band gap of about 6 eV, ranging from 4 eV below to 2 eV above the Fermi level of Ag(001), is observed.[18] The concentration of point defects on these films was estimated to be ∼0.1% of a ML.[19] For MgO thin films grown on Fe(001), a thickness dependence of the MgO band gap, which increases from 5 eV for 2 ML to 7.6 eV for 6 ML MgO, was reported by Klaua et al.[21] These authors reported also the presence of defect energy levels within the band gap of the MgO film, which give rise to increased tunneling current at negative bias voltage. A detailed microscopic investigation of defects on the MgO surface was, however, not possible so far. In the present letter, we report on

* Corresponding author. E-mail: sterrer@fhi-berlin.mpg.de.
† Fritz-Haber-Institut der Max-Planck-Gesellschaft.
‡ University of Wroclaw.
§ Universita degli Studi Milano-Bicocca.

10.1021/jp056306f CCC: $33.50 

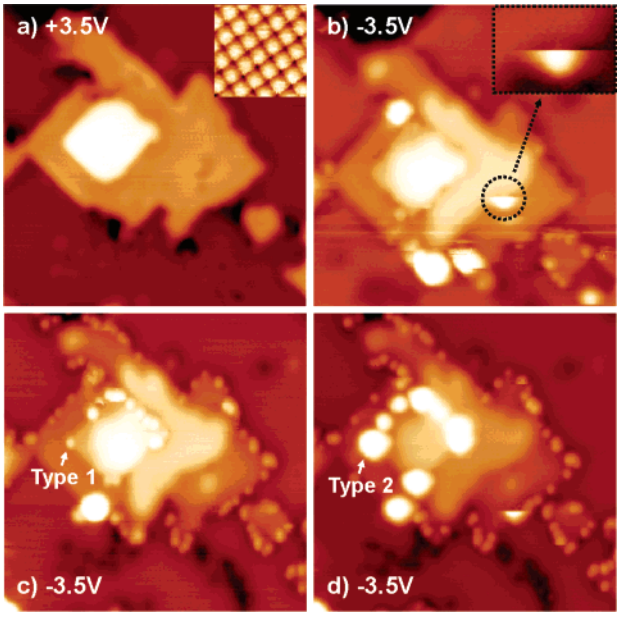


**Figure 1.** STM images ($25 \times 25$ nm$^2$, $I_t = 100$ pA) of a MgO island on 4 ML MgO(001)/Ag(001): (a) $V_S = +3.5$ V (the inset shows the atomic resolution on a MgO terrace ($15 \times 15$ Å$^2$)); (b) $V_S = -3.5$ V (the inset shows the magnification of the region, where a defect is changed during scanning); (c and d) images taken at $V_S = -3.5$ V, after subsequent scanning at high positive bias voltages.

a combined STM and STS study of localized defects on the surface of a 4 ML thin MgO(001) film grown on Ag(001). We show for the first time that two types of defects with different charge states exist on the surface and assign them, in corroboration with calculated data, to surface color centers.

Experiments were performed in a custom-built Eigler style ultrahigh vacuum (UHV) low-temperature scanning tunneling microscope with a double quartz tuning fork sensor for operation of the microscope in both STM and AFM mode.[22] The Ag(001) substrate was cleaned by repeated $Ar^+$ sputtering (800 V, 10 $\mu$A) and subsequent annealing to 700 K. MgO films were grown by reactive deposition of Mg in an oxygen pressure of $1 \times 10^{-6}$ mbar at a substrate temperature of 550 K. The MgO deposition rate was 0.75 ML/min. STM measurements were carried out at 5 K. For the spectroscopic characterization of the defects, $dz/dV_S$ (tip−sample separation vs sample bias voltage) spectra were recorded with a closed feedback loop. The calculations are based on an embedded cluster method[23] using the density functional theory (DFT) B3LYP exchange-correlation functional[24,25] and the 6-31G basis set. The cluster is divided into two main regions. One contains the quantum-mechanical (QM) cluster surrounded by interface ions (Mg*, described by an effective core potential) and by a region of classical shell model polarizable ions. All centers in this region are fully relaxed. The second region is represented by ±2 point charges fixed at the lattice positions which reproduce the long-range electrostatic potential. This scheme is implemented in the GUESS code[23] interfaced with Gaussian 98.[26] The terrace and step F centers were modeled by $Mg_{14}O_{13}Mg_{16}$* and $Mg_{11}O_{10}$-$Mg_{13}$* QM clusters, respectively. The relative positions of the defect-induced states with respect to the valence and conduction band edges have been determined from the energies of the corresponding Kohn−Sham levels.

In Figure 1, we show STM images of 4 ML MgO(001)/Ag(001) at different bias voltages. The best morphological characterization of the MgO film is obtained at high positive bias voltages when tunneling into the MgO conduction band takes place (Figure 1a, $V_S = +3.5$ V).[18] The overall morphology of the MgO film is comparable to results reported earlier for thinner MgO layers grown on Ag(001).[18−20] In general, the islands are square-shaped and oriented along the {100} directions. At a bias voltage of −3.5 V, we observe bright spots on the edges of the MgO islands additional to the MgO morphological features (Figure 1b). At negative bias voltages, tunneling occurs from filled Ag states into empty states of the tip. Under these tunneling conditions, an ideal epitaxial MgO film has no states contributing to the tunneling current that could give rise to the observed protrusions. The appearance of bright protrusions, which is equivalent to an increased conductance, gives an indication of the presence of localized defect states within the band gap of the MgO film.[21]

Similar defects were also observed by STM on MgO thin films that have been subjected to electron bombardment.[27] From electron energy loss (EEL) spectra[15] as well as metastable impact electron spectroscopy (MIES) studies[28] of electron bombarded MgO thin films, it is well established that electron bombardment leads to the formation of color centers. The increased conductance found in STM for defects at energies below the Fermi level ($E_F$) is in agreement with the observation of a peak at about 2 eV below $E_F$ in MIES spectra of electron bombarded MgO.[28] Unlike the studies mentioned above, in the present case, surface charging is mediated by the local electric field between the scanning tunneling microscope tip and the sample that provides the electronic and geometrical requirements for localization of electrons at specific surface sites. This is seen in Figure 1b for the defect in the center, which is changed during scanning (see inset), as well as in the STM images in Figure 1c and d that have been subsequently obtained on the same surface area as that in Figure 1b and which show an increasing concentration of defect states. The possibility of a tip-induced formation of defects was shown previously for $SiO_2$, where electron traps are formed locally by applying high bias voltages between the scanning tunneling microscope tip and the sample.[29]

In Figure 1, two types of defects can be distinguished on the MgO surface: those which appear as pointlike states (Figure 1c, type 1) and those giving rise to large and bright protrusions (Figure 1d, type 2). A comparison of, for example, the left corner on the upper MgO island in Figure 1c and d shows that both types of defects may be stabilized on one and the same surface location. This coincidence points to the fact that the two defect appearances are due to different charge states of one and the same defect type. Additionally, the defects are located at different possible sites on the step edges of the MgO islands, for example, at regular steps, kinks, or corners. From calculations, it is known that both the charge state and the location of color centers significantly influence their electronic properties.[12] To determine the site-specific electronic properties of single defects experimentally, we report in the following tunneling spectroscopic measurements for defects, which are discriminated by their different surface location as well as different appearance in STM images.

In Figure 2, the edge of a MgO island on 4 ML MgO(001)/Ag(001) is shown. The image taken at +3.5 V (Figure 2a), reflecting the morphology of this area, shows a straight step edge on the left-hand side, a perfect step corner, and an irregular step edge on the right-hand side. At a sample bias of −3.5 V, localized defects (type 1) appear on the step edges and on the corner site. In Figure 2b, constant current and corresponding conductance images at selected bias voltages obtained from the same area are displayed. In constant current mode, the integral density of states from the Fermi level ($E_F = 0$ V) to the selected

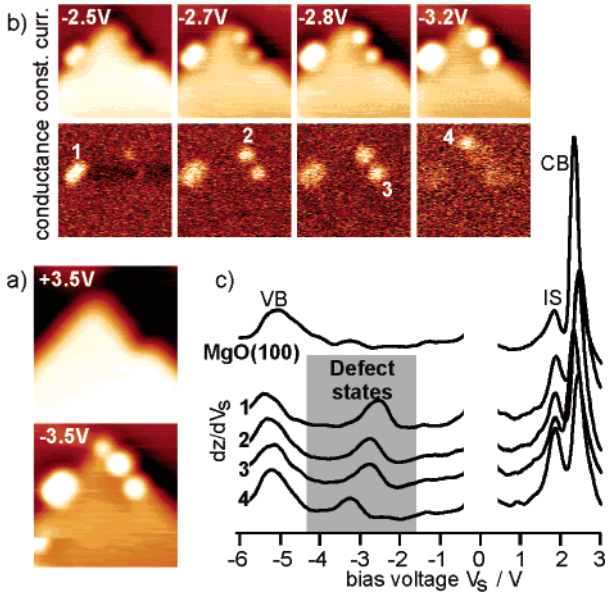


**Figure 2.** (a) STM images ($5 \times 5$ nm$^2$, $I_t = 100$ pA) of the morphology (at $V_S = +3.5$ V) and defect structure (at $V_S = -3.5$ V) of a MgO island on 4 ML MgO(001)/Ag(001). (b) Constant current and conductance images of defects located on the edges of a MgO island. (c) $dz/dV_S$ spectra taken on the perfect MgO(001) island and at the defect locations.

bias voltage ($V_S$) contributes to the image, whereas, in the differential conductance mode ($dI/dV_S$), the local density of states at the particular energy is imaged. The maximum conductance of different defects clearly depends on the applied bias voltage, being lowest for the defects located on the left-hand step edge ($-2.5$ V) and highest for the step corner ($-3.2$ V). Our observation of defect-mediated conductivity at negative bias voltages (tunneling out of filled sample states) points to the fact that the defects are related to occupied electron trapping sites with energy levels in the band gap of MgO.

Information on the electronic properties of the defects gained so far gives only their position relative to the Fermi level of the Ag(001) substrate. To locate the defect energy levels with respect to the electronic states of MgO, we recorded tunneling spectroscopy with a closed feedback loop ($dz/dV_S$ spectra) in a large bias range on the defect sites and the regular MgO(001) surface. The results are shown in Figure 2c. The topmost spectrum taken on an ideal MgO terrace shows characteristic features of the MgO film. The onset of the valence band (VB) and conduction band (CB) is observed at $-4.5$ and $+2.2$ V, respectively. An additional small peak at $+1.8$ V is due to the MgO$-$Ag interface state (IS). This spectrum well reproduces the results obtained earlier by Schintke et al. on the same system.[18,19] Spectra taken at defect sites 1$-$4 show additional peaks within the band gap of MgO between $-2.5$ and $-3.2$ V, in accordance with the conductance images shown above. The energy levels of type 1 defects are located about 1$-$2 eV above the valence band of MgO. Their position depends on the location of the defect on the surface and shifts toward the valence band when going from the edge to the corner site.

A characterization of type 2 defects is reported in Figure 3. At $V_S = +3.0$ V, the STM image shows the morphology of the surface area. A number of defects of both type 1 and type 2 appears at a bias voltage of $-3.5$ V. Defect states of type 2 imaged as large protrusions at $-3.5$ V are also recognizable at $+0.1$ V, whereas type 1 defects are not visible at this tunneling voltage. The location of electronic states in the MgO band gap is obviously different for type 1 and type 2 defects. A typical

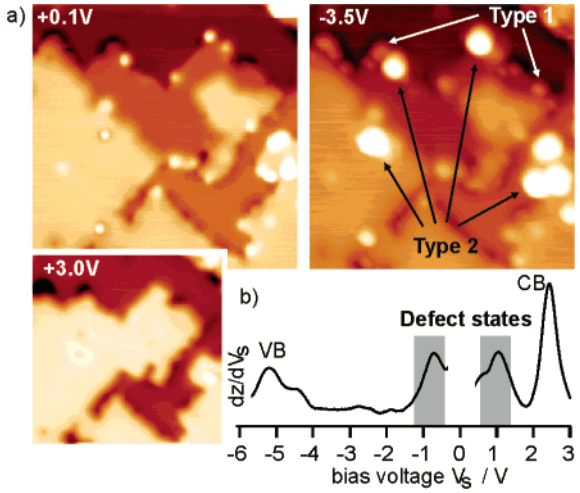


**Figure 3.** (a) Constant current STM images ($20 \times 20$ nm$^2$, $I_t = 50$ pA) at different bias voltages showing the distribution of charged defects on the surface of MgO(001) thin films. (b) $dz/dV_S$ spectrum taken at a type 2 defect.

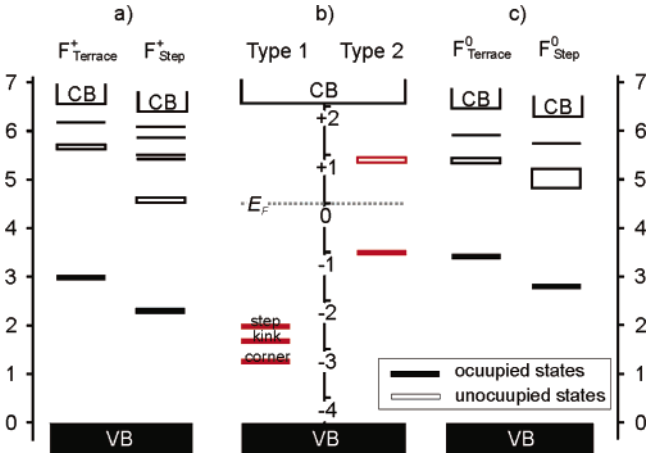


**Figure 4.** (a) Calculated energy levels of $F^+$ centers on terrace and step sites. (b) Summary of energy levels of type 1 and type 2 defects from STM experiments. (c) Calculated energy levels of $F^0$ centers on terrace and step sites.

tunneling spectrum of a type 2 defect is shown in Figure 3b. In contrast to the results in Figure 2c, we observe two peaks within the band gap of MgO, at around $-1$ and $+1$ V.[30] The peak at negative bias voltage originates from tunneling out of occupied defect states and is located in the middle between the valence band and the conduction band, whereas the peak at positive bias corresponds to tunneling into unoccupied defect states. For type 2 defects, no clear dependence of energy levels on the morphology was found.

To corroborate the assignment of the observed defects to color centers, we compare the experimental results with calculated ground state energy levels of $F^0$ and $F^+$ centers located at terraces and monoatomic steps. Neutral F centers ($F^0$, Figure 4c) present a doubly occupied state 3.4 eV (terrace) and 2.8 eV (step) above the top of the O 2p valence band. Above this state, there is a group of three empty close-lying electronic states. They are observed at 1.9$-$2.0 and 2.0$-$2.4 eV above the doubly occupied state on the terrace and step, respectively. $F^+$ centers (Figure 4a) present a singly occupied state 3.0 eV (terrace) and 2.3 eV (step) above the top of the valence band. For the terrace, a set of three empty states due to the charged vacancy is found at 2.6$-$2.7 eV above the filled level. On the step, the first empty level is at 2.3 eV above the singly occupied state. Two other levels are found at higher energies, 3.1 and 3.2 eV, respectively.

For comparison, the energy levels of type 1 and type 2 defects obtained from the tunneling spectra in this study are plotted in Figure 4b. We find good qualitative agreement between the calculated energy levels of occupied states for singly charged ($F^+$) and neutral ($F^0$) color centers and type 1 and type 2 defects, respectively. Unoccupied states are not observed for type 1 defects because of the location of the respective state for step $F^+$ centers close to the Fermi level of the MgO(001)/Ag(001) system, which prevents the experimental observation of this state. The dependence of the defect state location in the band gap on the coordination number found for $F^+$ centers (Figure 4a and ref 12) is also reproduced for type 1 defects, where the occupied state of the corner defect is located closer to the valence band than that of the step site. It should be noted here that the comparison of calculated and experimental data shown in Figure 4 has to remain qualitative, since the presence of the image charge in the Ag(001) substrate, as well as band bending effects due to the electric field between the scanning tunneling microscope tip and the sample, which is not taken into account in the calculations, might, to some extent, influence the position of the defect states.

In conclusion, the results presented in this study give the first combined microscopic and spectroscopic evidence for the presence of color centers on the MgO surface. Singly and doubly occupied color centers were identified by their specific appearance in STM images as well as by spectroscopic data revealing the electronic structure of the respective defects.

**Acknowledgment.** M.S. is grateful for financial support by the Austrian Science Fund (FWF). M.N. is indebted to the University of Wroclaw for financial support. G.P. is grateful to the A. von Humboldt Foundation for supporting his visit at the FHI in Berlin. This work was partially supported by the European Union through the STREP program GSOMEN. We are grateful to Emile Rienks for critical reading of the manuscript.

## References and Notes

(1) Wertz, J. E.; Auzins, P.; Weeks, R. A.; Silsbee, R. H. *Phys. Rev.* **1957**, *107*, 1535.

(2) Henderson, B.; King, R. D. *Philos. Mag.* **1966**, *13*, 1149.

(3) Nelson, R. L.; Tench, A. J. *J. Chem. Phys.* **1964**, *40*, 2736.

(4) Paganini, M. C.; Chiesa, M.; Giamello, E.; Coluccia, S.; Martra, G.; Murphy, D. M.; Pacchioni, G. *Surf. Sci.* **1999**, *421*, 246.

(5) Chiesa, M.; Paganini, M. C.; Giamello, E.; Di Valentin, C.; Pacchioni, G. *Angew. Chem., Int. Ed.* **2003**, *42*, 1759.

(6) Chiesa, M.; Paganini, M. C.; Spoto, G.; Giamello, E.; Di Valentin, C.; Del Vitto, A.; Pacchioni, G. *J. Phys. Chem. B* **2005**, *109*, 7314.

(7) Sterrer, M.; Berger, T.; Diwald, O.; Knözinger, E. *J. Am. Chem. Soc.* **2003**, *125*, 195.

(8) Sterrer, M.; Berger, T.; Stankic S.; Diwald, O.; Knözinger, E. *ChemPhysChem* **2004**, *5*, 1695.

(9) Sterrer, M.; Diwald, O.; Knözinger, E.; Sushko, P. V.; Shluger, A. L. *J. Phys. Chem. B* **2002**, *106*, 12478.

(10) Yoon, B.; Hakkinen, H.; Landman, U.; Worz, A. S.; Antonietti, J. M.; Abbet, S.; Judai, K.; Heiz, U. *Science* **2005**, *307*, 403.

(11) Sousa, C.; Pacchioni, G.; Illas, F. *Surf. Sci.* **1999**, *429*, 217.

(12) Suhsko, P. V.; Gavartin, J. L.; Shluger, A. L. *J. Phys. Chem. B* **2002**, *106*, 2269.

(13) Scorza, E.; Birkenheuer, U.; Pisani, C. *J. Chem. Phys.* **1997**, *107*, 9645.

(14) Ricci, D.; DiValentin, C.; Pacchioni, G.; Sushko, P. V.; Shluger, A. L.; Giamello, E. *J. Am. Chem. Soc.* **2003**, *125*, 738.

(15) Kramer, J.; Tegenkamp, C.; Pfnür, H. *Phys. Rev. B* **2003**, *67*, 235401.

(16) Ashworth, T. V.; Pang, C. L.; Wincott, P. L.; Vaughan, D. J.; Thornton, G. *Appl. Surf. Sci.* **2003**, *210*, 2.

(17) Barth, C.; Henry, C. *Phys. Rev. Lett.* **2003**, *91*, 196102.

(18) Schintke, S.; Messerli, S.; Pivetta, M.; Patthey, F.; Libioulle, L.; Stengel, M.; Vita, A. D.; Schneider, W.-D. *Phys. Rev. Lett.* **2001**, *87*, 276801.

(19) Schintke, S.; Schneider, W.-D. *J. Phys.: Condens. Matter* **2004**, *16*, R49.

(20) Valeri, S.; Altieri, S.; del Pennino, U.; di Bona, A.; Luches, P.; Rota, A. *Phys. Rev. B* **2002**, *65*, 245410.

(21) Klaua, M.; Ullmann, D.; Barthel, J.; Wulfhekel, W.; Kirschner, J.; Urban, R.; Monchesky, T. L.; Enders, A.; Cochran, J. F.; Heinrich, B. *Phys. Rev. B* **2001**, *64*, 134411.

(22) Heyde, M.; Kulawik, M.; Rust, H.-P.; Freund, H.-J. *Rev. Sci. Instum.* **2004**, *75*, 2446.

(23) Suhsko, P. V.; Shluger, A. L.; Catlow, C. R. A. *Surf. Sci.* **2000**, *450*, 153.

(24) Becke, A. D. *J. Chem. Phys.* **1993**, *98*, 5648.

(25) Lee, C.; Yang, W.; Parr, R. G. *Phys. Rev. B* **1988**, *37*, 785.

(26) Frisch, M. J.; Trucks, G. W.; Schlegel, H. B.; Scuseria, G. E.; Robb, M. A.; Cheeseman, J. R.; Zakrzewski, V. G.; Montgomery, J. A., Jr.; Stratmann, R. E.; Burant, J. C.; Dapprich, S.; Millam, J. M.; Daniels, A. D.; Kudin, K. N.; Strain, M. C.; Farkas, O.; Tomasi, J.; Barone, V.; Cossi, M.; Cammi, R.; Mennucci, B.; Pomelli, C.; Adamo, C.; Clifford, S.; Ochterski, J.; Petersson, G. A.; Ayala, P. Y.; Cui, Q.; Morokuma, K.; Malick, D. K.; Rabuck, A. D.; Raghavachari, K.; Foresman, J. B.; Cioslowski, J.; Ortiz, J. V.; Stefanov, B. B.; Liu, G.; Liashenko, A.; Piskorz, P.; Komaromi, I.; Gomperts, R.; Martin, R. L.; Fox, D. J.; Keith, T.; Al-Laham, M. A.; Peng, C. Y.; Nanayakkara, A.; Gonzalez, C.; Challacombe, M.; Gill, P. M. W.; Johnson, B. G.; Chen, W.; Wong, M. W.; Andres, J. L.; Head-Gordon, M.; Replogle, E. S.; Pople, J. A. *Gaussian 98*, revision A.6; Gaussian, Inc.: Pittsburgh, PA, 1998.

(27) Sterrer, M.; Fischbach, E.; Risse, T.; Freund, H.-J. *Phys. Rev. Lett.* **2005**, *94*, 186101.

(28) Kolmakov, A.; Stultz, J.; Goodman, D. W. *J. Chem. Phys.* **2000**, *113*, 7564.

(29) Watanabe, H.; Fujita, K.; Ichikawa, M. *Appl. Phys. Lett.* **1998**, *72*, 1987.

(30) The interface state cannot be resolved in the spectra in Figure 3b because of overlap with the defect peak.